Supporting Information

Effect of pH on the incorporation of acrylic acid units in the core of polymer nanoparticles prepared by PISA and on their morphology

Clément Debrie,[1] Noémie Coudert,[2] Jean-Michel Guigner,[3] Fanny Coumes,[1] Clément Guibert,[4] Simon Harrisson,[5] François Stoffelbach,[1] Olivier Colombani,[2*] Jutta Rieger[1*]

[1] Sorbonne Université & CNRS (UMR 8232), Institut Parisien de Chimie Moléculaire (IPCM), Polymer Chemistry Team, 4 Place Jussieu, 75252 Paris Cedex 05, France. jutta.rieger@sorbonne-universite.fr

[2] Le Mans Université & CNRS (UMR 6283), Institut des Molécules et Matériaux du Mans (IMMM), Avenue Olivier Messiaen, 72085 Le Mans Cedex 9, France. olivier.colombani@univ-lemans.fr

[3] Sorbonne Université, MNHN, CNRS (UMR 7590), Institut de Minéralogie, de Physique des Matériaux et de Cosmochimie (IMPMC), IRD, 75252 Paris Cedex 05, France

[4] Sorbonne Université & CNRS (UMR 7197), Laboratoire de Réactivité de Surface, 4 Place Jussieu, 75252 Paris Cedex 05, France

[5] Université de Bordeaux, Bordeaux-INP & CNRS (UMR 5629), Laboratoire de Chimie de Polymères Organiques, 16 Avenue Pey Berland, 33067 Pessac Cedex, France

I. Materials

Ethyl 2-(butylthiocarbonothoylthio)propanoate (CTA-1) was synthesized following already established protocols[1]. 1,3,5-Trioxane (Aldrich, 99 %), 2,2'-azobis(2-methylpropionitrile) (AIBN, ≥ 98%, Aldrich), 4,4'-azobis(4-cyanopentanoic) acid (ACPA, Aldrich, ≥ 98 %), 2,2'-azobis[2-(2-imidazolin-2-yl)propane]dihydrochloride (VA-044, Aldrich, 98 %), trimethylsilyldiazomethane (TMS, Acros, 2 M in hexane), *N*,*N*-dimethylformamide (DMF, VWR, Normapur), methanol (MeOH, Carlo Erba, > 99 %) and tetrahydrofuran (THF, VWR, pure) were used as received.

N,*N*-Dimethylacrylamide (DMAc, Aldrich, > 99 %), acrylic acid (AA, Aldrich, 99 %) and 2-methoxyethylacrylate (MEA, Aldrich, 98 %) were distilled under reduced pressure to remove radical scavengers from the commercial monomers. Deionized water was used for all polymerizations. Concentrated hydrochloric acid (HCl, VWR, 36 %) was diluted with water and sodium hydroxide (NaOH, Acros Organics, 98.5 %) was dissolved in water to provide solutions of known concentration to modify α in PISA or post-polymerization dispersions.

II. Methods

^{1}H NMR.

Monomer conversions were followed by ^{1}H NMR in D_2O or acetone-d_6 for DMAc, in acetone-d_6 for MEA and AA during PISA, using 1,3,5-trioxane as an internal reference. All analyses were recorded at room temperature with a Bruker 300 or 400 MHz spectrometer in 5-mm diameter tubes.

Dynamic Light Scattering analyses (DLS).

Dynamic Light Scattering (DLS) measurements were carried out on a Zetasizer Nano S90 from Malvern (90° angle, 5 mW He–Ne laser at 633 nm) to determine the z-average particle diameter (D_z) of diluted dispersions in water at C = 1 g·L^{-1}.

Size Exclusion Chromatography (SEC).

SEC analyses were carried out on two PSS GRAM 1000 Å columns (8 × 300 mm; separation limits: 1 to 1000 $kg \cdot mol^{-1}$) and one PSS GRAM 30 Å column (8 × 300 mm; separation limits: 0.1 to 10 $kg \cdot mol^{-1}$) coupled with a differential refractive index detector (RI) and a UV detector (λ = 309 nm, maximal absorption of the trithiocarbonate moiety). Dimethylformamide (+ LiBr 1 $g \cdot L^{-1}$) at 60 °C was used as the mobile phase at a flow rate of 0.8 $mL \cdot min^{-1}$. Samples were prepared at a concentration around 5 $mg \cdot mL^{-1}$ and filtered through a 0.20 µm pore-size PTFE membrane before the injection (V_{inj} = 100 µL). The number-average molar mass (M_n), the weight-average molar mass (M_w) and the dispersity ($Đ = M_w/M_n$) were calculated from the RI signals with OmniSEC 5.12 software thanks to a conventional calibration curve based on PMMA standards.

Before injection, to avoid interaction with the column, the AA units of the copolymers were methylated.[2] The polymers were dried and dissolved in THF/MeOH (90/10 v/v) at around 2 $mg \cdot mL^{-1}$. A few droplets of HCl (1 M) were added in the solution to ensure acidic conditions and thereby complete protonation of the AA units. Thereafter, TMS in hexane was added dropwise until nitrogen bubbling stopped and the solution remained slightly yellow. Solvents and excess TMS were evaporated under air flux.

Comment: We note that the molar masses obtained correspond to PMMA-equivalent values rather than true values. Determining true molar masses would have required using a combination of light scattering and refractive index detection and to determine the refractive index increment of the polymers, which depends on their compositions. However, such information would not have changed the qualitative conclusions and therefore only PMMA-equivalent values are provided.

Determination of the individual conversions for MEA and AA.

Small aliquots of the polymerization medium were regularly taken, dissolved in acetone-d_6 and analyzed by ^1H NMR. Upon increasing α, the signals of the vinylic protons of AA were shifted to lower chemical shifts because AA is globally more-electron-rich. The chemical shift of **c'** proton is relatively pH-insensitive whereas the two other protons are greatly affected by α.[3] Thus, the signals of the vinylic protons of MEA and AA are either well separated, at high enough α, or overlaid at α close to 0 (see **Figure S1**).

For α >> 0, at time *t*, individual conversions x_{MEA} and x_{AA} could be calculated from the integrals (*I*) of the vinylic protons of each monomer (*I* of proton **a'** for AA and *I* of proton **a** for MEA) as follows, using trioxane as an internal reference (δ ≈ 5.11 ppm):

$$x_{AA,t} = 1 - \frac{I_{AA,t}}{I_{AA,0}}$$

When α ~ 0, the global conversion (x_{global}) could be estimated by integrating the whole vinylic signal (5.8 – 6.4 ppm). The conversion in AA (x_{AA}) was then estimated by integrating the partial signal of one vinylic proton of AA, which was identifiable at 6.26 ppm. The conversion in MEA (x_{MEA}) was calculated with the following formula:

$$x_{MEA} = \frac{x_{global} - x_{AA}\, f_{AA,0}}{1 - f_{AA,0}}$$

where $f_{AA,0}$ is the molar fraction of AA at t = 0 determined by the introduced masses of monomers.

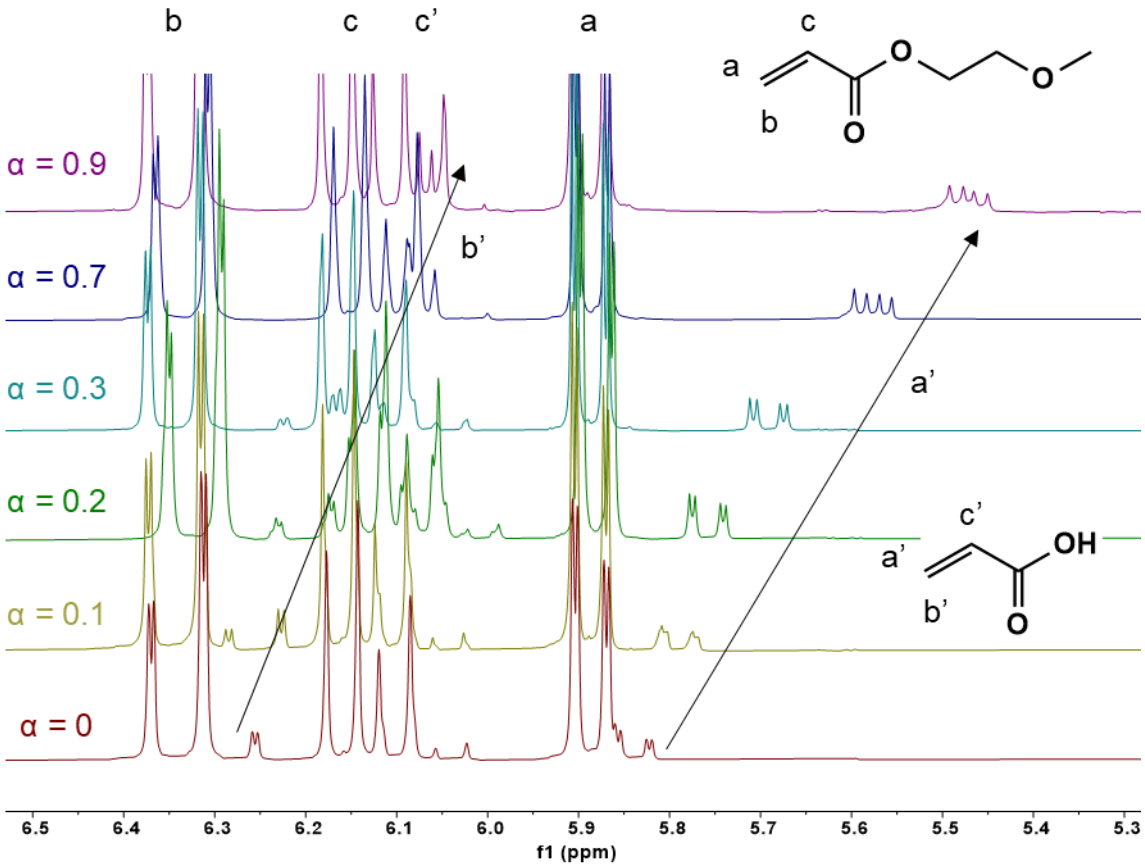

Figure S1. ^{1}H NMR in acetone-d_6 of MEA and AA aqueous mixtures at different α and at typical PISA concentrations [AA] ≈ 5 g·L^{-1} (here f_{AA} = 0.05).

Calculation of the degree of ionization of AA, α.

α was determined using the experimental masses of AA and the volume of the NaOH solution used. The latter (C = 1.000 M) was titrated twice using the solid non-hygroscopic monoacid hydrogen potassium phthalate[4] to confirm its concentration. α was thus given by:

$$\alpha = \frac{n_{NaOH}}{n_{AA,0}}$$

We stress that the definition of α given above actually corresponds to the *degree of neutralization* from a strict point of view, that is the number of AA units transformed into sodium acrylate units. Because of counter-ions condensation in polyelectrolytes, some of the sodium acrylate units for strong ions pairs with their counter-ion and do not really express their charges.[5] However, for weakly ionized polyelectrolytes such as the P(MEA-*co*-AA) copolymers which contain up to 30 mol% AA, the counter-ion condensation should remain weak so that the approximation "*degree of neutralization*" ≈ "*degree of ionization*" is a reasonable approximation.

The natural value of α (when no NaOH is added) is referred to as $\alpha_0 \sim 0$ in this work for the sake of simplicity. α_0 is however not strictly equal to 0 and can be calculated from the initial concentration in AA, C_0, and the pK_a of AA/AA^- using the following formula:

$$\alpha_0 = \frac{\sqrt{K_a^2 + 4K_aC_0} - K_a}{2C_0}$$

With $K_a \approx 8 \cdot 10^{-5}$[3] and typical concentrations C_0 ranging from $7.5 \cdot 10^{-2}$ to $4.5 \cdot 10^{-1}$ $mol \cdot L^{-1}$, it can be approximated by:

$$\alpha_0 \approx \sqrt{\frac{K_a}{C_0}}$$

Thus, the "natural" α_0 is 0.01-0.03, depending on the concentration of AA.

Changing α post-polymerization.

Generally, the required amount of NaOH (1M solution) was calculated based on the chemical structure of the polymer, and NaOH additions were performed to polymer dispersions at 50 $g \cdot L^{-1}$. For the DLS analyses, α was adjusted on 1 $g \cdot L^{-1}$ aqueous solutions, to which small volumes of NaOH were progressively added.

Cryo-Transmission Electron Microscopy (cryo-TEM).

Polymer solutions were prepared at 3 wt% in water by diluting the reaction mixture to this concentration. 3 µL of the aqueous solutions (at 3 wt%) were then deposited on a quantifoil grid. Excess solution was removed with Whatman filter paper and the grid was immediately frozen in liquid ethane. The observations were carried out at -180 °C by a JEOL JEM-2100 LaB_6 microscope operating at 200 kV. The images were taken on a Gatan US1000, 2k x 2k CCD Camera.

Small Angle X-ray Scattering (SAXS).

SAXS measurements were performed on the SWING beamline of the SOLEIL Synchrotron (Saint Aubin, France) in four series at energies of 12 keV (λ = 1.03 Å) or 7 keV (λ = 1.77 Å). See **Table S1** for configuration details. An exposure time of 1 s and a gap time of 500 ms were used with a two-dimensional CCD detector (EigerX4M in vacuum, 162.5 × 155.2 mm^2, pixel size: 75 × 75 μm^2).

Table S1. Configurations of the beamline used for SAXS measurements in the SOLEIL Synchrotron.

#Run	Date	E (keV)	$D_{sample\text{-}detector}$ (mm)	q_{min} ($Å^{-1}$)	q_{max} ($Å^{-1}$)
1	April 2021	7	2131	$1.75\ 10^{-3}$	$3.13\ 10^{-1}$
2	Oct. 2021	12	3534	$1.81\ 10^{-3}$	$3.22\ 10^{-1}$
3	Sept. 2022	12	6237	$1.17\ 10^{-3}$	$1.78\ 10^{-1}$
4	April 2023	12	1907	$4.78\ 10^{-3}$	$5.70\ 10^{-1}$

The measurements were done at 25 °C, unless stated otherwise. For several samples, measurements were performed at different temperatures using a thermostated capillary holder device (the targeted temperature being maintained for 3–5 min prior to measurements) at concentrations varying from 1 to 200 $g \cdot L^{-1}$, typically at 50 $g \cdot L^{-1}$. Standard correction procedures were applied for X-ray beam transmission, detector efficiency, and signal subtraction of the 1.5 mm capillary filled with the solvent. The software packages Foxtrot was used to achieve this data reduction. The data were fitted using the SasView software (http://www.sasview.org/). According to the observed morphologies using cryo-TEM, the data were fitted with the form factor of either spheres with radius R_s[6], cylinders with Radius R_c and length l [7], or vesicles with internal radius R_c and thickness e[6] (see **Figure S2** for a representation of the models). Note that the lamella model (L) corresponds to an infinite or planar vesicle (infinite R_c).

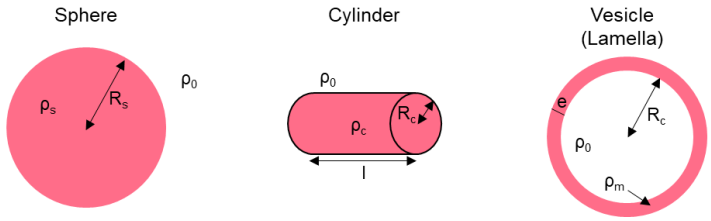

Figure S2. Schematic representation of the models used in SasView software.

In most cases, the characteristic sizes of the nano-objects are dispersed. A lognormal distribution function was then used to consider the variability of the dimensions of the self-assemblies. Note that for such distribution, SasView gives the median value and σ is related to the width of the distribution. When the fit was good without dispersity or with very small σ values ($\sigma < 0.01$), the dimensions determined are assumed to be monodisperse and mentioned as "m" in the tables gathering the fitting parameters.

III. Syntheses

III.1. PDMAc macroCTA-1 and PDMAc macroCTA-2

The synthesis of PDMAc macroCTA-1 was carried out in DMF solution and described elsewhere.[8] Its characteristics are summarized in **Table S2**. PDMAc macroCTA-2 was synthesized in aqueous solution. However, as CTA-1 is not water-soluble, the reaction was started in bulk and water was added later, as follows.

In a 25 mL round-bottom flask, 0.385 g (1.44 mmol) of CTA-1, 4.013 g (40.5 mmol) of DMAc, 0.395 g (4.38 mmol) of 1,3,5-trioxane and 0.040 g (0.14 mmol) of ACPA were introduced and degassed under argon in an ice bath for 45 min. The flask was immersed in an oil bath heated at 60 °C. After 15 min of reaction, 16 mL of previously degassed water was introduced in the flask and the oil bath was heated up to 70 °C. The conversion in DMAc was then followed by ^{1}H NMR in D_2O by taking small aliquots from the flask. The reaction was stopped after 107 min by immersing the flask in an ice bath and opening it to air. The solution was dialyzed against water using 500 Da SpectraPor® RC-membrane during 24 h and then freeze-dried to provide 4.05 g of a yellow powder. The solid was characterized by ^{1}H NMR in D_2O and SEC. A number-average degree of polymerization of DP_n = 25.5 and thus, a number-average molar mass of M_n = 2.80 kg·mol^{-1}was determined by ^{1}H NMR (see **Figure S3**). The results are summarized in **Table S2**.

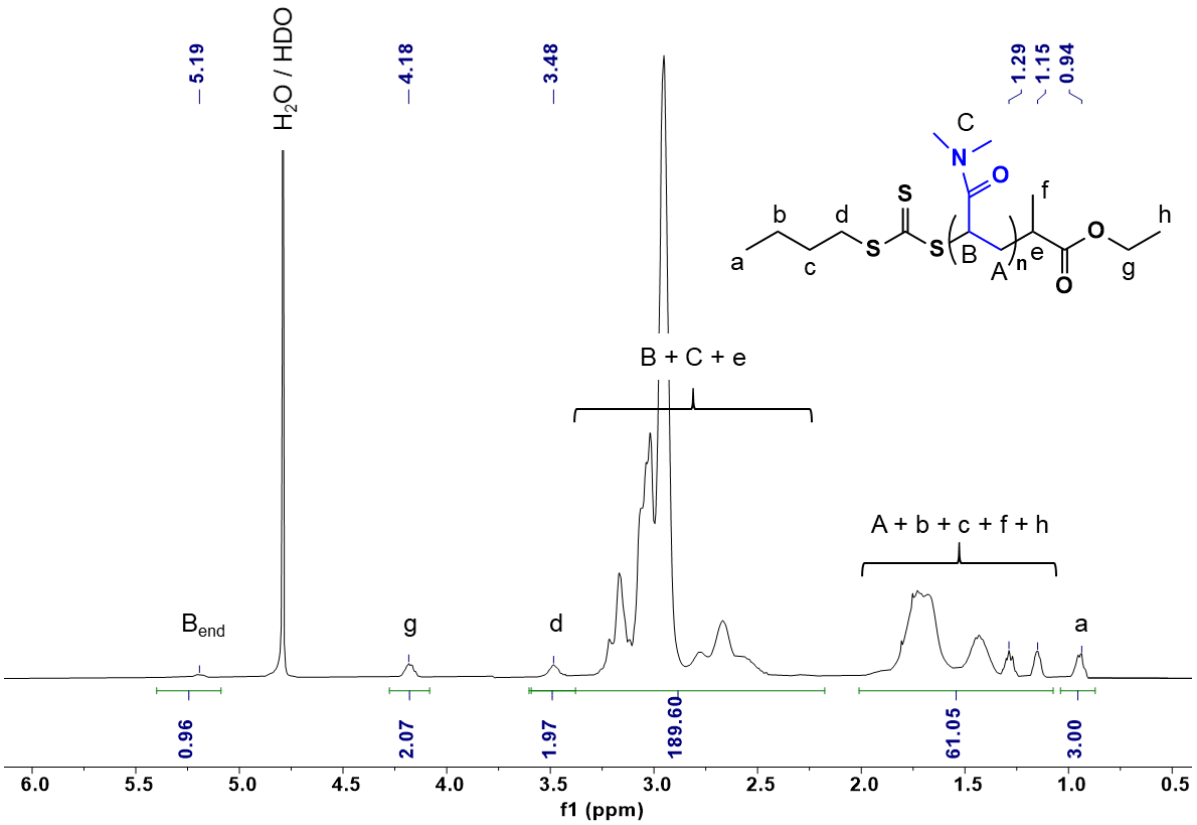

Figure S3. ^{1}H NMR of the pure PDMAc macroCTA-2 recorded in D_2O.

Table S2. Synthesis conditions and characteristics of the PDMAc macroCTA-1 and -2.

#	$[CTA]_0/[DMAc]_0/[I]_0$ [1]	Time (min)	Conv[2] (%)	$DP_{n,conv}$ [3]	$M_{n,conv}$ [3] (kg/mol)	$DP_{n,NMR}$ [4]	$M_{n,NMR}$ [4] (kg/mol)	$M_{n,SEC}$ [5] (kg/mol)	$Đ$ [5]
macroCTA-1	1/35.7/0.10	72	79	28.2	3.06	24.1	2.65	2.32	1.13
macroCTA-2	1/28.0/0.10	107	91	25.6	2.81	25.5	2.80	2.28	1.10

[1] Initial molar ratios of CTA/DMAc/initiator (AIBN for macroCTA-1 and ACPA for macroCTA-2) introduced. [2] Monomer conversion at the end of the polymerization, determined by ^{1}H NMR using trioxane as internal reference. [3] Number-average degree of polymerization, DP_n, and number-average molar mass, M_n, calculated using the experimental conversion. [4] Number-average degree of polymerization, DP_n, and number-average molar mass, M_n, determined by ^{1}H NMR. [5] Number-average molar mass, M_n, and dispersity $Đ$ determined by SEC in DMF (+ LiBr 1 g·L^{-1}) using PMMA calibration.

III.2. PDMAc-*b*-P(MEA-*co*-AA) at α ~ 0

Protocol

In a typical experiment (Entry 200-10 in **Table S3**), 51.3 mg (19.1 µmol) of macroCTA-1, 29.0 mg (0.316 mmol) of trioxane, 0.444 g (3.41 mmol) of MEA, 0.544 g (0.404 mmol) of a solution of AA in water (0.163 g of AA dissolved in 2.886 g of water), 0.133 g (1.91 µmol) of a solution of VA-044 in water (9.3 mg of VA-044 dissolved in 1.991 g of water) and 1.372 g of water were introduced in a 5 mL round-bottom flask. The reaction medium was degassed under argon bubbling for 40 min in an ice bath before being immersed in an oil bath pre-heated at 40 °C. Small aliquots of the polymerization medium were regularly taken to determine the conversions in MEA and AA by ^{1}H NMR. After 7h30 of reaction, the flask was cooled down in an ice bath and opened back to air to stop the reaction. The dispersion was used without further purification for DLS, SAXS and cryo-TEM characterizations, and after drying and methylation for SEC.

Table S3. Syntheses and characterizations of PDMAc-*b*-P(MEA-*co*-AA) copolymers synthesized at α ~ 0.

#[1]	#macro CTA	$[I]_0/[macro\ CTA]_0$[2]	R[2]	$f_{AA,0}$[2]	Reaction time	Conv.[3] MEA/AA	$DP_{n,\ conv}$[4]	$F_{AA,\ conv}$[4]	$M_{n,\ conv}$[4] (kg/mol)	$M_{n,\ SEC}$[5] (kg/mol)	$Đ$[5]	D_z[6] (nm)	Morpho.[7]
150-0	1	0.11	154	0	6h43	95	147	0	21.8	25.4	1.08	37	S
200-0	1	0.10	209	0	4h41	95	200	0	28.6	37.4	1.11	49	S
250-0	1	0.24	254	0	22h23	99	251	0	35.3	45.5	1.17	52	S
300-0	1	0.11	301	0	4h37	95	286	0	39.9	52.8	1.12	107	V
400-0	1	0.11	405	0	6h44	93	378	0	51.8	70.2	1.13	138	V
150-5	2	0.13	148	0.049	6h07	97/93	144	0.047	21.1	21.8	1.09	70	S (+F)
250-5	1	0.14	248	0.051	5h51	96/92	239	0.049	33.1	42.3	1.13	89	V
300-5	1	0.11	305	0.050	15h45	99/99	303	0.050	41.2	54.8	1.17	120	V
420-8	1	0.09	415	0.078	6h09	96/88	396	0.071	52.6	70.8	1.15	209	V (+ L)
150-10*	1	0.10	153	0.098	6h07	91/82	137	0.089	19.8	27.2	1.13	36	sF
200-10	1	0.10	200	0.106	7h30	89/77	175	0.093	24.5	30.6	1.09	206	F
250-10	1	0.12	248	0.102	15h42	99/99	246	0.101	33.2	46.9	1.15	236	V (+ S)
290-10	1	0.13	293	0.096	7h00	92/88	268	0.091	36.1	40.6	1.18	259	V
250-15	1	0.11	249	0.155	7h01	94/87	231	0.146	30.8	42.8	1.13	199	V
150-30	2	0.11	145	0.286	9h23	97/93	139	0.279	18.6	19.6	1.09	118	sF
150-30bis*	1	0.10	149	0.295	6h21	90/78	128	0.266	17.4	24.0	1.12	-	-
200-30	1	0.10	199	0.309	21h43	97/93	191	0.301	24.1	33.1	1.09	616	V (+ L)
250-30	1	0.14	250	0.303	6h30	93/85	227	0.283	28.5	41.5	1.11	> 1000	V + L
310-30	1	0.23	314	0.313	24h19	100/98	311	0.309	37.6	51.5	1.24	595	V + L

* Synthesis carried out at a solids content of 10 wt%, instead of 20 wt%. [1] Samples are named R-$f_{AA,0}$ where R is the initial molar ratio of monomers with respect to the macroCTA, and $f_{AA,0}$ the molar content (in %) of AA introduced in the monomer feed. [2] Initial molar ratios introduced. I = VA-044; R = $[monomer(s)]]_0/[macroCTA]_0$; $f_{AA,0}$ is the initial molar content in AA. [3] Final monomer conversions determined by ^{1}H NMR using trioxane as internal reference. [4] Molar content in AA in the hydrophobic block (F_{AA}), its number-average degree of polymerization, $DP_{n,\ B}$, and number-average molar mass of the diblock copolymer, M_n, calculated using the experimental individual conversions. [5] Number-average molar mass, M_n, and dispersity $Đ$ determined by SEC in DMF (+ LiBr 1 g·L^{-1}) using a PMMA conventional calibration. [6] Z-average diameter measured by DLS at C = 1 g·L^{-1} and 25 °C (after storing the sample at 5°C). [7] Morphology of the nano-objects as determined by cryo-TEM imaging. S = spheres, sF = short fibers, F = fibers, V = vesicles, L = lamellae. The minor morphologies is indicated in brackets.

Kinetic monitoring and control over the copolymerization

By SEC a shoulder at the higher molar masses side was detected on the SEC RI signal that shifted towards higher values with increasing conversion (**Figure 1** in main article). The shoulder was much less intense on the UV-Vis detector (set at 309 nm, *i.e.* the maximum of TTC absorption), suggesting that it stems mainly from termination reactions by chain recombination which lead to a loss of the TTC end-group.

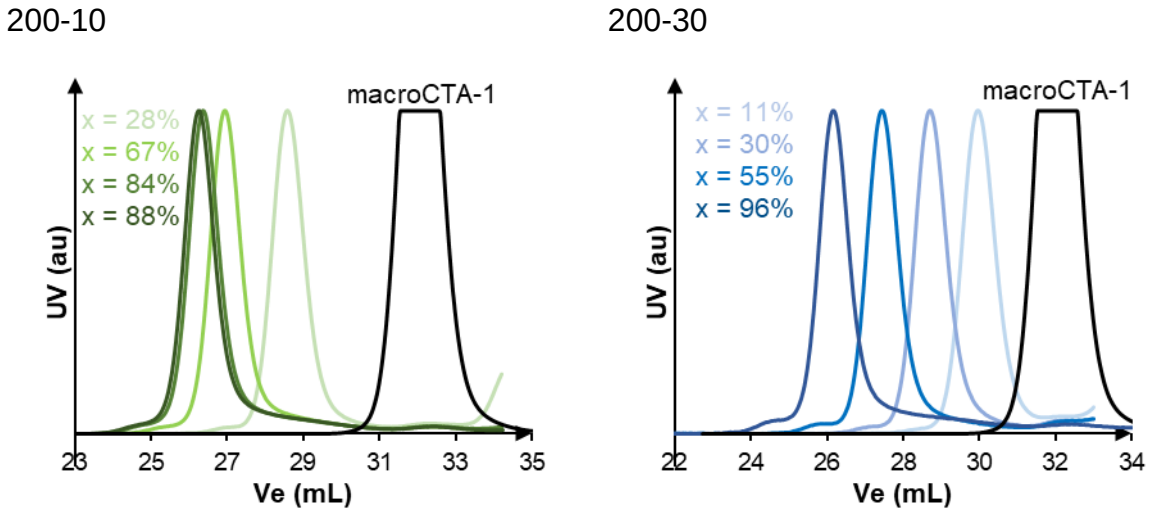

Figure S4. Overlay of the normalized SEC UV (309 nm) traces for the kinetic monitoring of samples 200-10 and 200-30 (**Table S3**).

Additional SEC traces

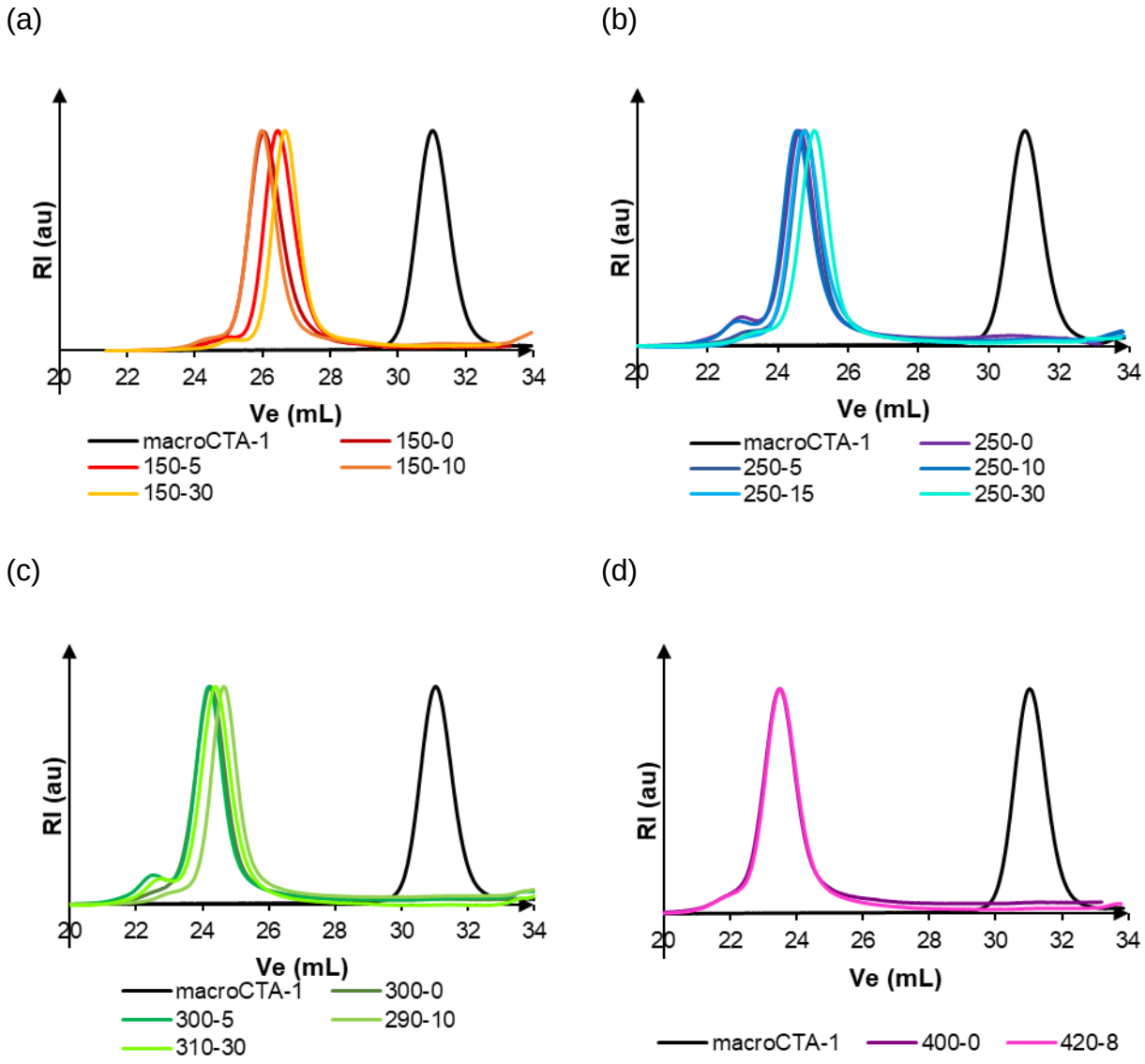

Figure S5. SEC traces for the series synthesized at $R \approx$ (a) 150, (b) 250, (c) 300 and (d) 400.

Additional SAXS traces

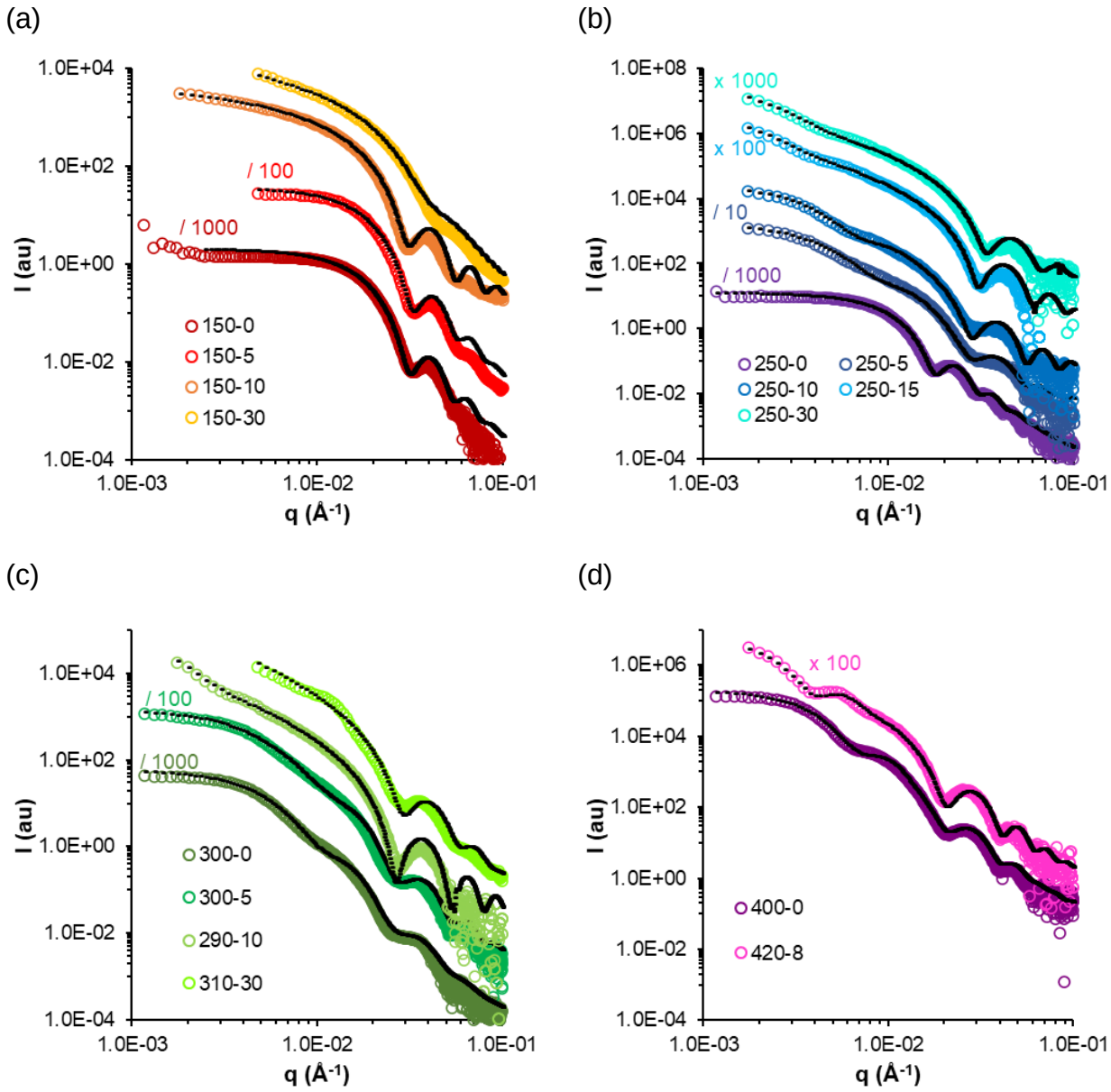

Figure S6. Effect of the incorporation of AA in the PMEA block: SAXS traces for the series synthesized at $R \approx 150$ (a), (b) $R \approx 250$, (c) $R \approx 300$ and (d) $R \approx 400$. The black dotted lines are models fitting the experimental data, details in **Table S4**.

Additional cryo-TEM images

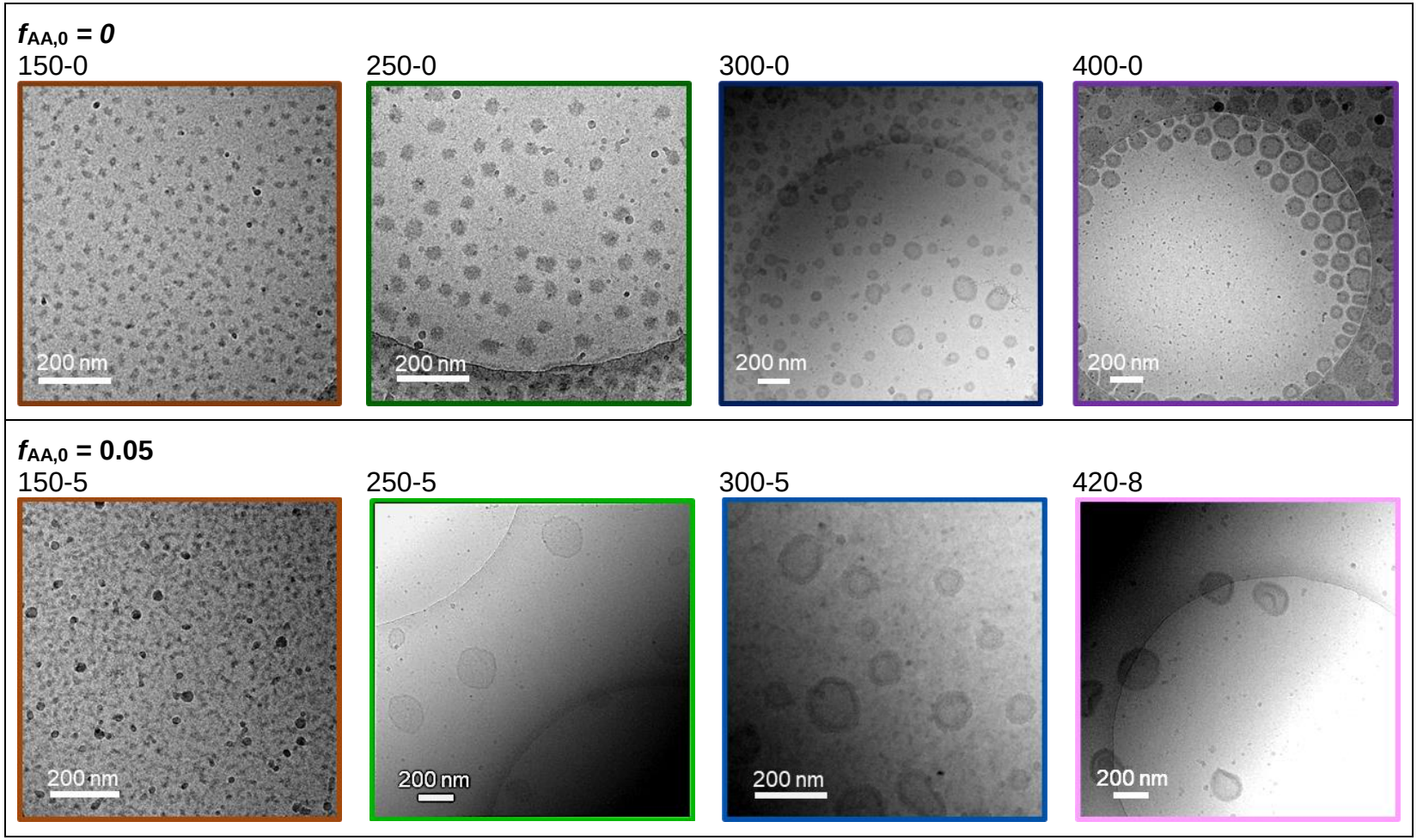

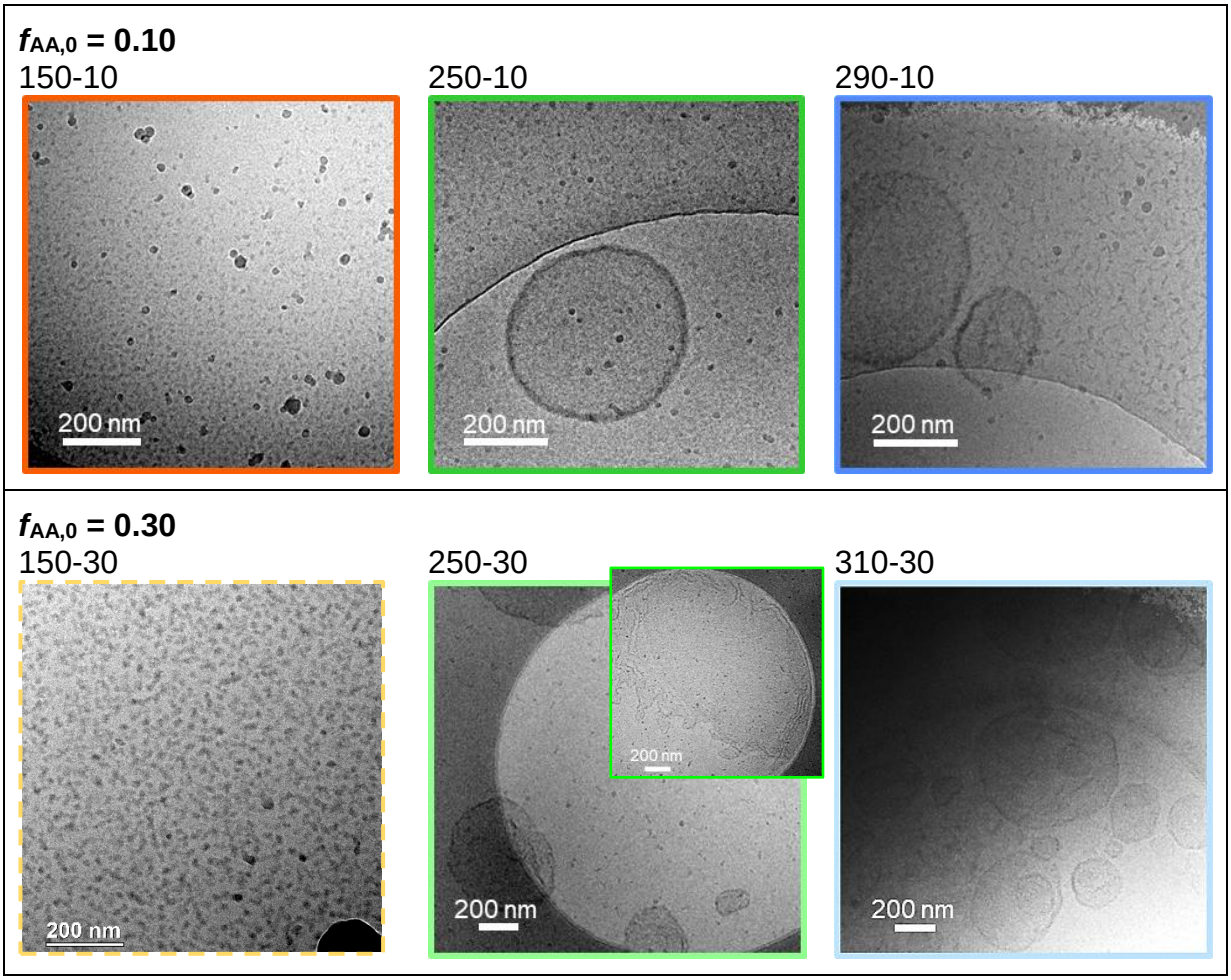

Figure S7. Effect of $f_{AA,0}$ and R: Representative cryo-TEM pictures of samples from the series synthesized with ≈ 150, 250, 300 and 400 synthesized at α ~ 0.

Series R = 250

Spheres were observed by cryo-TEM for sample 250-0 without AA, while vesicles were formed for $F_{AA} \geq 0.05$ (see **Figure S7**). SAXS fits confirmed the morphologies and indicated that the diameter of the self-assemblies increased from 50, to 83 and to 115 nm as F_{AA} was increased from 0 to 0.05 and 0.30, while the thickness of the membrane of the vesicles was similar independent of the AA content (*cf.* **Table S4**, for samples 250-5, 250-10, 250-15 and 230-30, the thickness was estimated at 23, 23, 21 and 19 nm, respectively).

Series R = 300

Vesicular and/or lamellar objects were always formed (**Figure S7**), *i.e.* no morphological change occurred when F_{AA} was increased from 0 to 0.30. However, D_z increased

with F_{AA} and the thickness of the double-membrane remained constant at around 25 nm according to SAXS (**Table S4**). This result is in agreement with the observation that the introduction of AA favors the formation of higher order morphologies, and the fact that the AA-free sample 300-0 ($PDMAc_{24}$-*b*-$PMEA_{290}$) already self-assembled into vesicles.

Summary of DLS, SAXS and cryo-TEM characterization results

Table S4. Morphology and geometrical parameters of the self-assemblies obtained by PISA at α ~ 0 determined by DLS, cryo-TEM and SAXS.

#[1]	D_z[1] (nm)	Morpho. TEM[2]	Morpho. SAXS[3]	D[4] (nm) (σ)	l or e[5] (nm) (σ)
150-0	37	S	S	28 (0.09)	-
200-0	49	S	S	30 (0.13)	-
250-0	52	S	S	50 (0.10)	-
300-0	107	V	V	72 (0.52)	24 (0.14)
400-0	138	V	V	110 (0.36)	32 (0.16)
150-5	70	S (+F)	S	27 (0.09)	-
250-5	89	V	V	83 (0.48)	23 (0.10)
300-5	120	V	V	70 (0.64)	24 (0.13)
420-8	209	V (+L)	V	174 (0.25)	31 (0.07)
150-10	36	sF	sF	25 (0.06)	61 (0.59)
200-10	206	F	F	28 (0.16)	> 100
250-10	236	V (+S)	V	99 (0.40)	23 (m)
290-10	259	V	V	170 (0.46)	24 (m)
250-15	199	V	V	141 (0.52)	21 (0.05)
150-30	118	sF	F	18 (0.23)	> 100
200-30	616	V (+L)	L	-	16 (0.14)
250-30	> 1000	L+V	V	115 (0.49)	19 (0.07)
310-30	595	L+V	L	-	24 (0.14)

[1] Sphere equivalent Z-average hydrodynamic diameter measured by DLS at C = 1 $g \cdot L^{-1}$ and 25 °C (after storing the sample at 5°C). [2] Morphology of the nano-objects identified on cryo-TEM pictures. The minor morphology is indicated in brackets. S = spheres, F = fibers, sF = short fibers, V = vesicles and L = lamellae. [3] Model used on SasView to fit the SAXS experimental data. [4] Diameter D and its 'lognormal polydispersity' σ of either spheres, cylinder or vesicle determined by fitting SAXS data. [5] Length l (for cylinders), membrane thickness e (for vesicles or lamellae) and their 'lognormal polydispersity' σ determined by fitting. m = monodisperse (σ < 0.01).

III.3. PDMAc-*b*-P(MEA-*co*-AA) at $\alpha > 0$

In a typical experiment (Entry A-1 in **Table S5**), 41.0 mg (14.4 µmol) of PDMAc macroCTA-2, 34.3 mg (0.374 mmol) of trioxane, 0.313 g (0.215 mmol) of a solution of AA in water (0.198 g of AA dissolved in 3.803 g of water) and 1.867 g of water were introduced in a 5 mL round-bottom flask. α was then increased by adding 34.2 µL (0.209 mmol) of a concentrated NaOH solution (6.124 M) with a micro-pipette and under vigorous stirring. Eventually, 538 mg (4.13 mmol) of MEA and 0.123 g (1.48 µmol) of a solution of VA-044 in water (15.1 mg of VA-044 dissolved in 3.863 g of water) were added in the reaction medium, before it was sealed and degassed under argon for 20 min. The flask was then immersed in an oil bath at 40 °C. Aliquots were regularly taken to determine the individual conversions in MEA and AA. After 22h53, the reaction was stopped by immersing the flask in an ice bath and opening it to air. The dispersion was ready to use for characterizations.

SEC traces of the series A-x

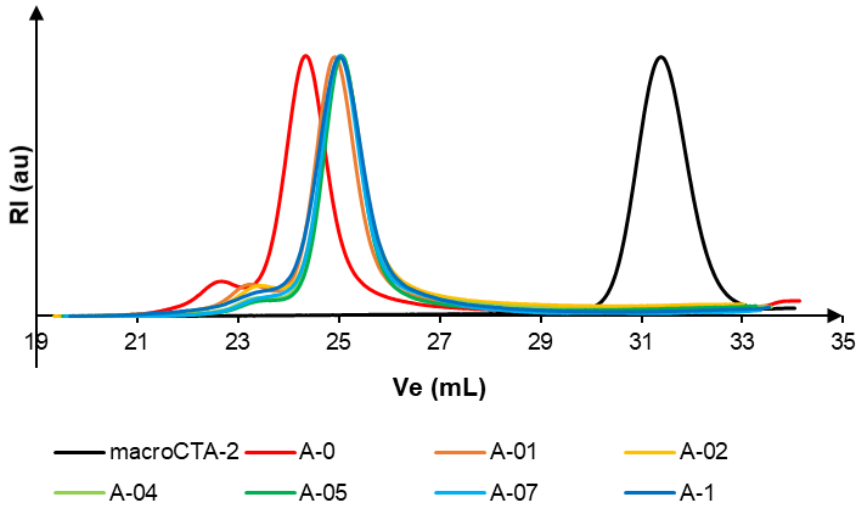

Figure S8. Overlay of normalized SEC traces of the samples of series A (from A-0 to A-1).

Comment: The small shoulder at higher molar masses is attributed to recombination reactions as its peak molar mass is double that of the main peak.

Table S5. Syntheses and characterizations of PDMAc-*b*-P(MEA-*co*-$AA_{0.05}$)$_{300}$ copolymers synthesized at different α.

#[1]	#macro-CTA	α_0 [2]	$[I]_0 / [\text{macro-CTA}]_0$ [3]	R [3]	$f_{AA,0}$ [3]	Time	Conv.[4]	$DP_{n,conv}$ [5]	$F_{AA,conv}$ [5]	N_{AA}/chain[6]	$M_{n,conv}$ [5] (kg/mol)	$M_{n,SEC}$ [7] (kg/mol)	$Đ$ [7]	D_z [8] (nm)	Morpho.[9]
A-0*	1	0.03	0.11	305	0.050	15h45	99/99	303	0.050	15.2	41.2	54.8	1.17	120	V
A-01	2	0.10	0.15	299	0.050	21h33	99/89	295	0.046	13.6	40.4	42.8	1.16	101	V(+F+S)
A-02	2	0.23	0.25	312	0.062	7h44	98/61	299	0.039	11.7	41.0	38.7	1.19	78	F(+S+V)
A-04	2	0.41	0.28	298	0.051	7h29	99/50	287	0.026	7.5	39.7	39.4	1.14	57	S+V
A-05	2	0.50	0.11	301	0.051	7h38	97/48	284	0.026	7.4	39.3	40.6	1.09	38	V(+S)
A-07	2	0.70	0.16	296	0.053	23h00	98/36	279	0.020	5.6	38.8	39.8	1.13	53	S
A-1	2	0.98	0.10	297	0.049	22h53	100/42	288	0.022	6.3	39.9	41.5	1.14	50	S

[1] Samples are named A-x where x is related to α_0 in the monomer feed. [2] Degree of ionization of AA moieties during the polymerization. [3] Initial molar ratios of VA-044 and monomers (R) introduced with respect to the macroCTA and initial molar content in AA. [4] Conversions in (MEA/AA) at the end of the polymerization determined by ^{1}H NMR using trioxane as internal reference. [5] Molar content in AA in the hydrophobic block (F_{AA}), its number-average degree of polymerization, $DP_{n,B}$, and number-average molar mass of the diblock copolymer, M_n, calculated using the experimental individual conversions. [6] Average number of AA units incorporated per polymer chain using the experimental conversions. [7] Number-average molar mass, M_n, and dispersity $Đ$ determined by SEC in DMF (+ LiBr 1 g·L^{-1}) using PMMA calibration. [8] Z-average diameter measured by DLS at C = 1 g·L^{-1} and 25 °C (after storing the sample at 5°C). [9] Morphology of the self-assemblies as determined by cryo-TEM (and confirmed by SAXS for almost all samples). The minor morphology is indicated in brackets. S = spheres, F = fibers, V = vesicles.* Sample A-0 corresponds to sample 300-5 reported in Table S3.

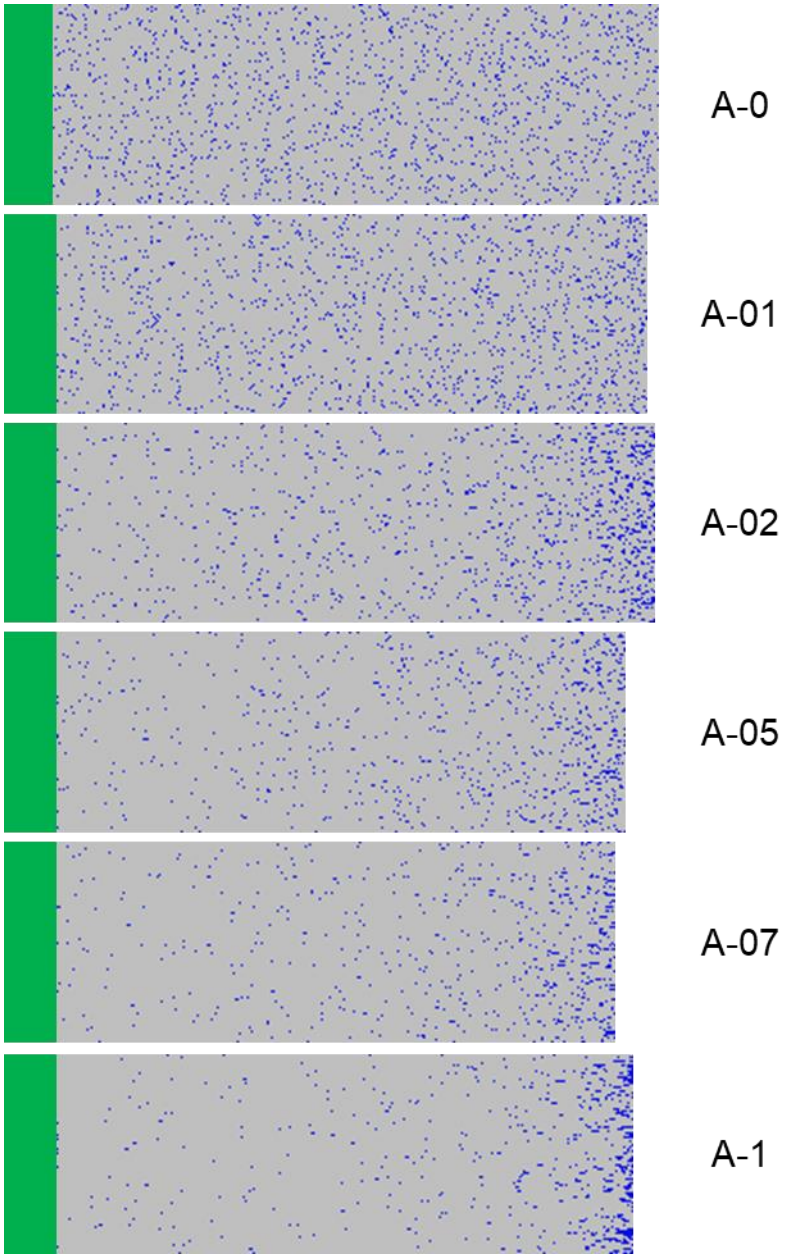

Figure S9. Simulation of 100 monodisperse PDMAc-*b*-P(MEA-*co*-AA) chains, stacked horizontally. The PDMAc block is represented in green, MEA in grey and AA units in blue. Each line on a figure corresponds to a different chain. The direction of polymerization is from left to right. Experimental $f_{AA,0}$, R, reactivity ratios of MEA and the final global conversion were used in the terminal model to determine the composition profiles.[9]

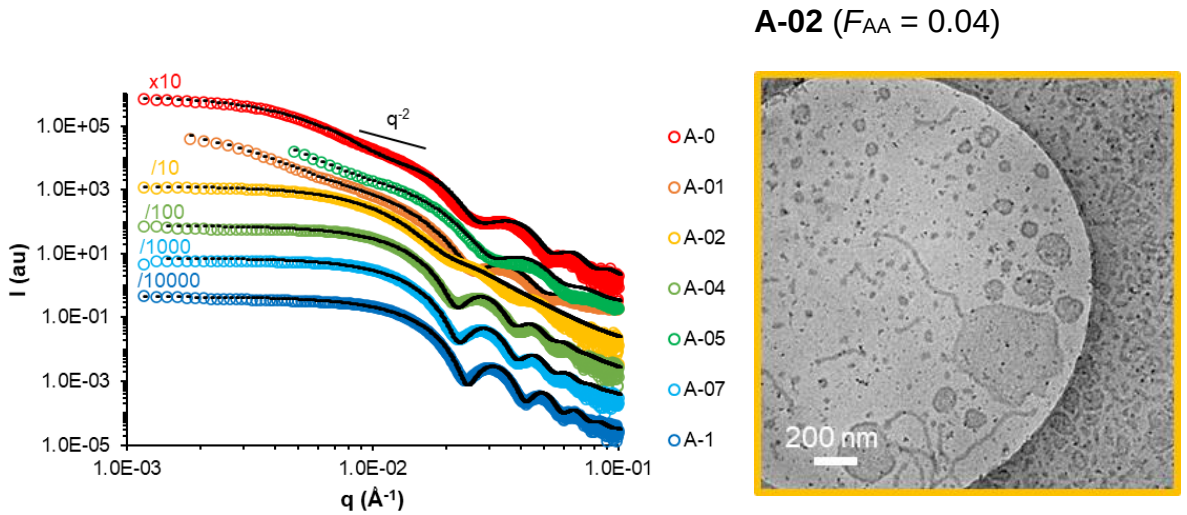

Figure S10. (left) SAXS data of samples of series A recorded at C = 30 g·L^{-1}. The black dotted lines are models fitting the data, see **Table S6** for details. (right) Cryo-TEM image (C = 30 g·L^{-1}) of sample A-02 (R = 300, $f_{AA,0}$ = 0.05).

Table S6. Geometrical parameters of the self-assemblies obtained by PISA at α > 0 using NaOH determined by SAXS at 30 g·L^{-1}.

#	Morpho. TEM[1]	Morpho. SAXS[2]	D[3] (nm) (σ)	e[4] (nm) (σ)
A-0 (=300-5)	V	V	70 (0.64)	24 (0.13)
A-01	V (+F+S)	V	101 (0.62)	25 (0.11)
A-02	F (+S+V)	(S)*	40 (0.24)	-
A-04	S+V	S	41 (0.09)	-
A-05	V (+S)	V	81 (0.54)	21 (0.13)
A-07	S	S	40 (0.08)	-
A-1	S	S	37 (0.07)	-

[1] Morphology of the nano-objects identified on cryo-TEM pictures. The minor morphology is indicated in brackets. S = spheres, F = fibers, V = vesicles. [2] Model used on SasView to fit the SAXS experimental data. [3] Diameter D and the 'lognormal polydispersity' σ of either spheres or vesicles determined by fitting the SAXS data. [4] Membrane thickness e (for vesicles) and its 'lognormal polydispersity' σ determined by fitting. *Sample A-02 could not be fitted well with simple fits, because it contains a complex mixture of morphologies as revealed by TEM (see Figure S10). As an example, a sphere fit is displayed in **Figure S10**.

IV. Response to α (modified post-polymerization)

We modified the degree of ionization of the AA units (α) post-polymerization and studied its effect on the morphology and solubility of the assemblies. The reversibility of the transitions was evaluated by increasing and re-decreasing α to its initial value.

DLS performed at different α at C = 1 g·L^{-1}

In order to determine the threshold values of F_{AA} and $DP_{n,B}$ at which chain dissociation occurs, a series of samples was analyzed in dilute conditions by DLS at C = 1 g·L^{-1} (*i.e.* 200 times less concentrated than in PISA). The samples were not filtered before measurement. The scattering intensities recorded as increasing amounts of NaOH were added are plotted in **Figure S11.** A strong decrease in the scattering intensity (reported here as derived count rate, DCR) with increasing α is observed for all samples studied. A DRC below 10 corresponds to values typically recorded for pure water or polymer solutions (unimers), and was considered to indicate aggregate dissociation into very small entities, probably unimers. Once such value was obtained, no reliable Dz could be measured.

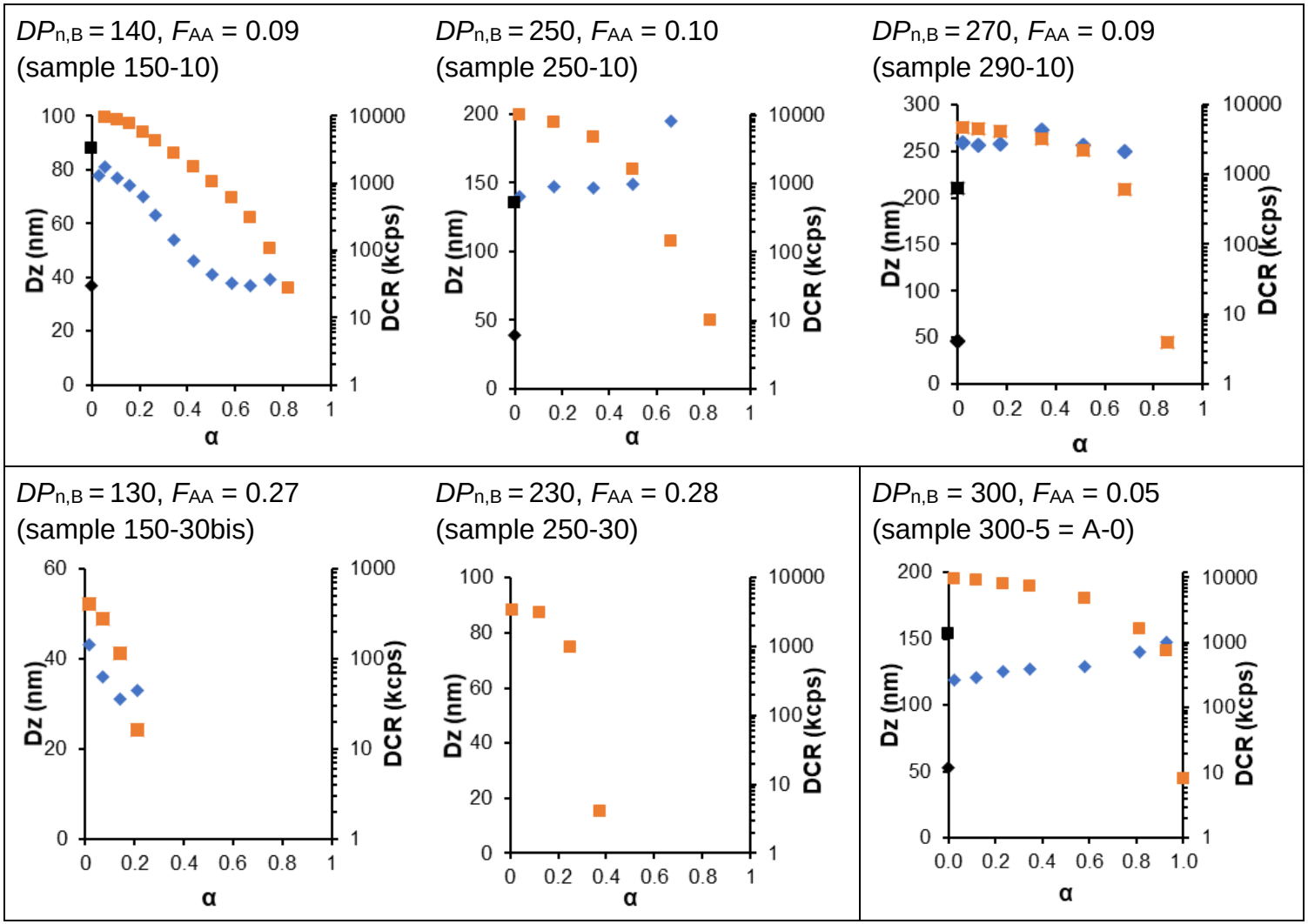

Figure S11. Evolution of the hydrodynamic diameter D_z (♦) and the intensity of scattered light (■) upon increasing progressively α from 0 to 1 post-polymerization (recorded at C = 1 g·L^{-1}, sample diluted immediately at the end of the polymerization). The symbols in black (♦, ■) at α = 0 indicate that α was set back to 0 (after having set it to 1).

SAXS analyses performed at different α at C = 50 g·L^{-1}

SAXS studies were used to monitor the effect of AA deprotonation on the assembly. At first, a series of samples synthesized at $\alpha_0 = 0$ was studied. In these samples the AA units are randomly distributed in the PMEA block. The effect of the ionization of the AA units was investigated by SAXS on 5 wt% samples to which small volumes of a NaOH solution (1 M) were added. **Figure 9** (in the main article) shows the SAXS data of sample 300-5 (= A-0 *vesicles*) to which no, 0.5 or 1 equivalent of NaOH (relative to the AA units) was added: increasing α from 0 to 0.5 induced a clear change in the slope at intermediate q (from q^{-2} to q^{0}) indicating a morphological transition from vesicles to spheres. Similar morphological transitions have been observed for PDMAc-*b*-P(CMAm-*co*-AA) vesicles also prepared by PISA.[10]

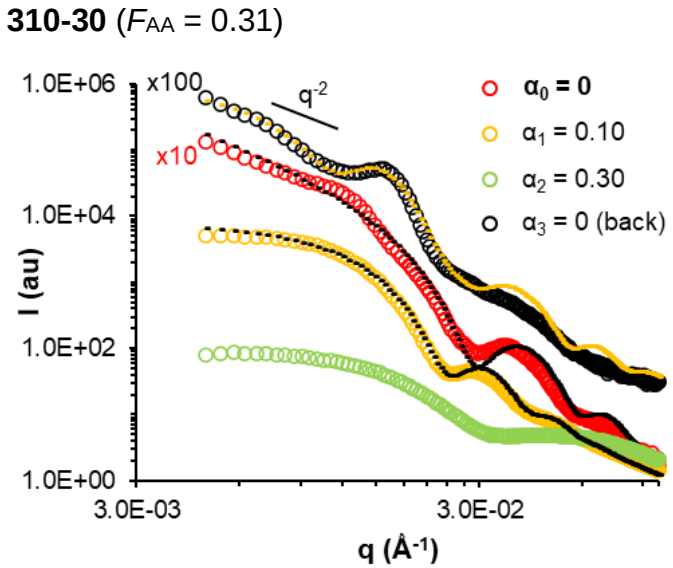

Figure S12. SAXS monitoring of the progressive deprotonation of the AA units of sample 310-30 (*lamellae*) (SAXS at C = 50 g·L^{-1}) and return to α = 0 (back). The black dotted lines are models fitting the data (see **Table S7**).

Sample 300-5. At α = 1, the 300-5 self-assemblies dissolved into unimers, When α was decreased back from α = 1 to 0, the scattering profile overlaid with that at α = 0.5, *i.e.* spheres quasi identical to those obtained at α = 0.5 were formed (black and green curves in **Figure 9,** D_{SAXS} = 38 vs. 41 nm, **Table S7**). This result suggests that the initial vesicles could not be reformed from the molecularly dissolved sample (unimers at α = 1). Morphological transitions can thus be induced by partial protonation, however the transitions from higher order to lower

order morphologies are not reversible. The pathway dependency of the morphologies suggests that frozen nano-objects are formed for 300-5.

In order to confirm the frozen character of 300-5 assemblies, we also tried to form the nano-objects from the solid state by direct dissolution in water. We therefore freeze-dried the initial PISA dispersion (300-5), and dissolved it afterwards in dichloromethane, which is a good solvent for both blocks, to erase any self-organization remaining from the initial state. A homogeneous dispersion could be formed by vigorous stirring of the dried sample in water at 20 wt% but the dispersion was unstable over time. Analysis of diluted samples by cryo-TEM revealed a complex mixture of large vesicles, long entangled fibers and spherical aggregates (**Figure S13**), confirming that sample 300-5 was not at thermodynamic equilibrium and the type of objects obtained is strongly pathway dependent.

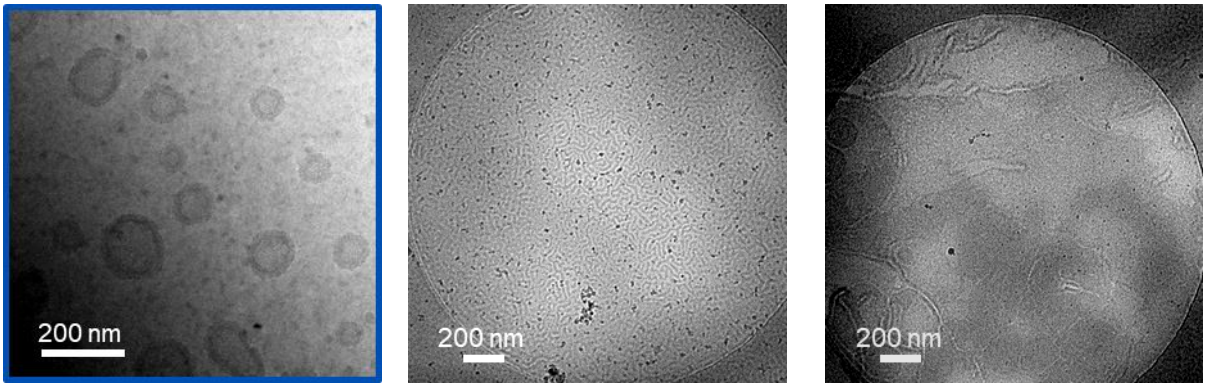

Figure S13. Representative cryo-TEM pictures of (left) pristine and (middle and right) re-dispersed samples 300-5. The dispersion of solid 300-5 (= A-0) in water was performed after full dissolution in dichloromethane and drying.

Sample 310-30. Successive deprotonation and reprotonation was also performed on sample 310-30 (*lamellae,* see cryo-TEM in **Figure S7**), which has a similar $DP_{n,B}$, but contains 6 times more AA (30 mol% AA, randomly distributed in the chain). The fitted SAXS data are presented in **Figure S12** and **Table S7**. The addition of only 0.1 equiv. of NaOH was sufficient to observe the change of the slope from q^{-2} towards q^{0} at low q values, indicating that the lamellar structures evolved towards spherical objects (**Table S7**, D = 36 nm). Moreover, the SAXS data suggested that the assemblies completely dissociated when 0.3 equiv of NaOH were added, as the scattered intensity was very low and did not exhibit any significant q-dependency (**Figure S12**). When α was reduced back to 0 (from α = 1), nano-objects reformed

and the SAXS data showed that complex morphologies (others than spheres) or a mixture of morphologies were formed, which were however not the same as the initial ones. This pathway dependency suggests again that the objects of sample 310-30 are not at thermodynamic equilibrium.

Sample 150-30. We also modified the degree of ionization of sample 150-30 (*short fibers*, **Table S4**). Again, the addition of 0.1 equivalents of NaOH induced a transition towards spherical objects (as suggested by the change of the slope at intermediate q values, see **Figure 11** top, in the main article) and the assemblies dissolved into unimers in the presence of 0.3 equiv. of NaOH. After complete dissolution, the addition of 1 equiv. of HCl led to a scattering profile which was similar to the initial one.

Responsiveness of polymers synthesized at $\alpha \neq 0$; Impact of the composition profile

The samples discussed above have been synthesized at $\alpha_0 = 0$, *i.e.* in conditions in which the AA units are randomly inserted in the copolymer. We had formerly shown[11,12] that the composition profile of statistical copolymers including AA units can have a great impact on their assembly. We studied the impact of the composition profile by comparing the effect of protonation on three copolymers possessing a similar $DP_{n,B}$ and low AA fractions (A-0, A-05, A-1 produced at $f_{AA,0} = 0.05$, see composition profile presented in **Figure 7** and **Figure S9**). The SAXS data are summarized in **Figure S14** and results of the fits reported in **Table S7**. SAXS analyses of sample A-1 synthesized at $\alpha = 1$ (PDMAc-*b*-(MEA-*co*-$AA_{0.022}$)$_{288}$) clearly suggests a morphological transition from spheres to vesicles, when the AA units are progressively protonated. This result is confirmed by cryo-TEM analyses (**Figure 10**). In contrast, the SAXS data of sample A-05 (PDMAc-*b*-(MEA-*co*-$AA_{0.026}$)$_{284}$) obtained at intermediate $\alpha = 0.5$ (mainly *vesicles*, **Figure S14**) remained quasi unchanged when α was decreased from 0.5 to 0, indicating that diminishing the degree of ionization had little impact on the self-assemblies. In contrast, when α was raised from 0.5 to 0.70 to 1, the SAXS data suggest a transition from vesicles to spheres to unimers, similar to sample A-0.

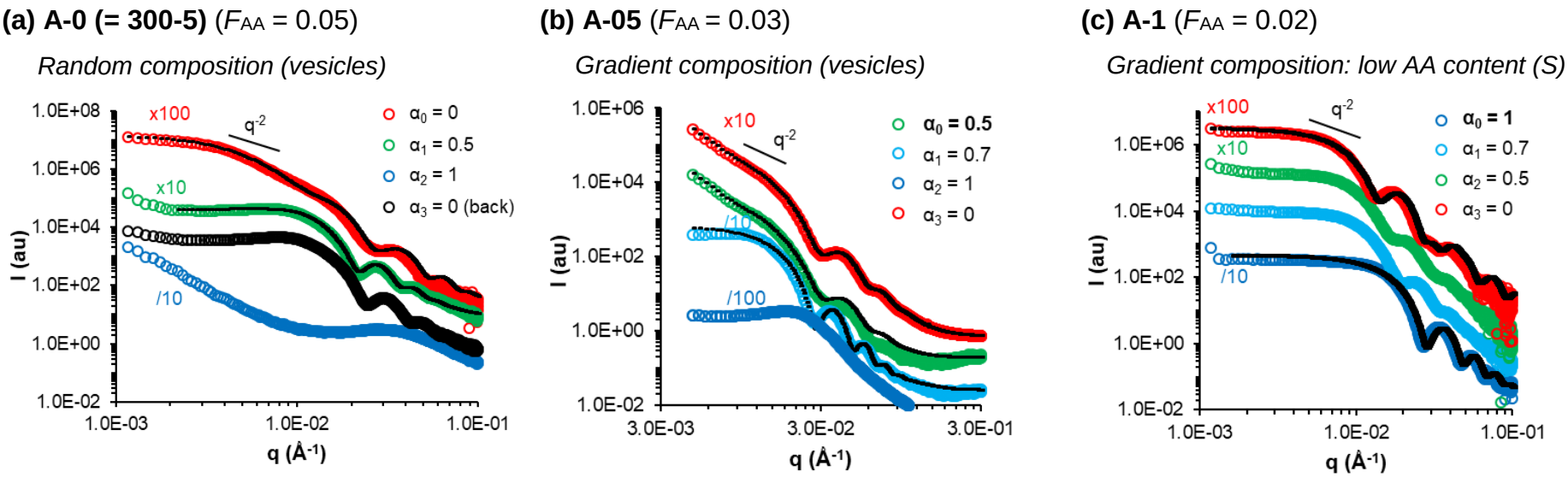

Figure S14. Overlay of SAXS data of samples (a) A-0 (= 300-5), (b) A-05 and (c) A-1 prepared at constant R = 300 and $f_{AA,0}$ = 0.05 but different α_0 (recorded at C = 50 g·L^{-1}). Effect of modifying α post-polymerization. The black dotted lines are models fitting the data (see **Table S7**).

Additional data attesting post-polymerization pH-sensitivity for samples synthesized at α ~ 0.

Table S7. Geometrical parameters of the self-assemblies determined by SAXS upon changing α at C = 50 g/L.

#	α[1]	Morpho. SAXS[2]	D[3] (nm) (σ)	l or e[4] (nm) (σ)
A-0 (= 300-5)	*0 (pristine)*	V	70 (0.64)	24 (0.13)
	0.1	V	84 (0.59)	27 (m)
	0.5	S*	41 (0.10)	-
	0 (back)	S*	38 (0.10)	-
150-5	*0 (pristine)*	S	27 (0.09)	-
	0.5	S*	21 (0.12)	-
150-30	*0 (pristine)*	F	18 (0.23)	≥ 100
	0.1	S*	19 (0.19)	-
	0 (back)	F	15 (0.45)	≥ 100
310-30	*0 (pristine)*	L	-	22 (0.11)
	0.1	S	36 (0.12)	-
	0 (back)	V*	70 (0.38)	23 (0.08)
A-05	*0.5 (pristine)*	V	81 (0.54)	21 (0.13)
	0	V	81 (0.58)	21 (0.12)
	0.7	S	32 (0.08)	-
A-1	*1 (pristine)*	S	37 (0.07)	
	0	V	61 (0.28)	21 (0.03)

[1] The degree of ionization of the AA units was adjusted, by addition of tiny volumes of NaOH or HCl concentrated solutions. The mention "pristine" indicates the α at which the nano-objects were synthesized and "0 (back)" means that α was successively increased to 1 and reduced back to 0. [2] Model used on SasView to fit the SAXS experimental data. S = spheres, V = vesicles and L = lamellae. [3] Diameter D and its 'lognormal polydispersity' σ of either spheres, cylinders or vesicles determined by fitting. [4] Length l (for cylinders), membrane thickness e (for vesicles or lamellae) and their 'lognormal polydispersity' σ determined by fitting. m = monodisperse (σ < 0.01). * For these fits, interactions between objects were considered and modelized by the use of a structure factor of hard spheres.

V. Response to temperature (modified post-polymerization)

PMEA exhibits LCST-like behavior in water.[13,11] A true LCST cannot be determined for PMEA because it is insoluble in water for most DP_n, concentrations and temperatures.[14] However, the critical transition temperature can be increased by copolymerizing MEA with a more hydrophilic comonomer like acrylic acid[11], 2-hydroxyethyl acrylate[15] or oligo(ethylene glycol)$_{8\text{-}9}$ acrylate[16]. We have recently demonstrated that P(MEA-*co*-AA) statistical copolymers are thermoresponsive and exhibit a LCST-type temperature transition that depends on both pH and the composition profile of the polymers.[11]

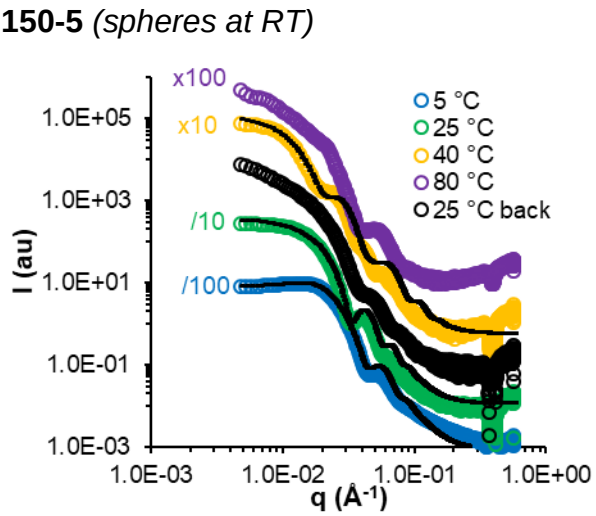

Figure S15. Temperature-controlled SAXS analyses of sample 150-5 analysed at α = 0. The black dotted lines are models fitting the data.

In contrast to samples 150-5 (**Figure S15**) and 150-30 (**Figure 9, right**), the SAXS analyses of sample 300-5 (= A-0, **Figure S14)**, which is constituted of vesicles at room temperature, did not reveal any morphological changes when heated. Instead, the diameter of the vesicles increased upon heating and the membrane thickness also increased from 18 nm at 5 °C to 48 nm at 80 °C (see **Table S8**). In a similar fashion, for sample A-1 (**Figure S14**), which was synthesized and analyzed at α = 1, the SAXS data indicate that spherical objects are maintained over the whole temperature range studied. The fits using a sphere model suggested again an increase of the diameter upon heating, notable from 30 to 46 nm when the temperature was increased from 5 to 80 °C. Diminishing α to 0.5 allowed sample A-1 to reorganize upon heating: it formed spheres at 25 °C but vesicles at 60 °C.

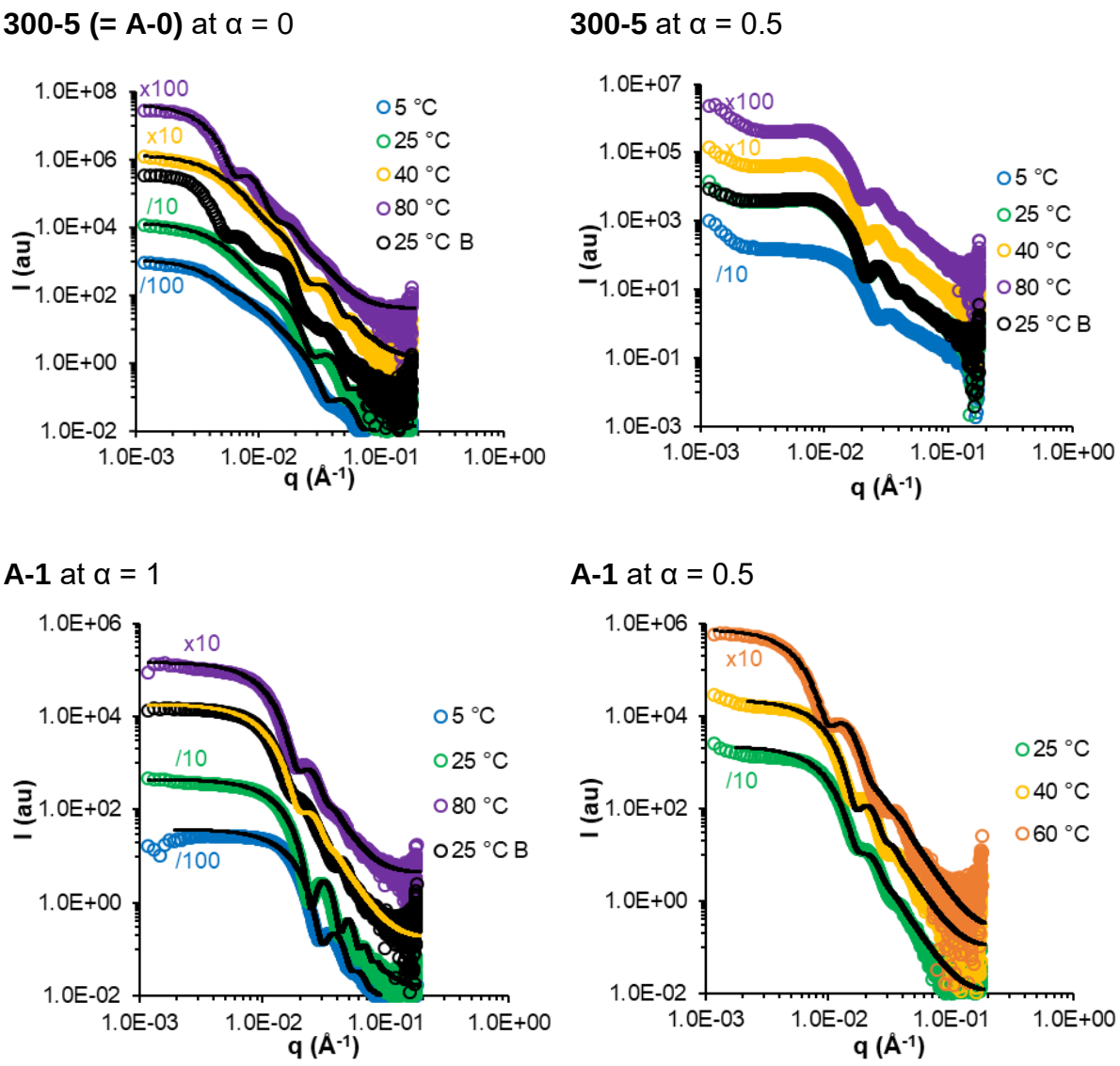

Figure S16. Temperature-controlled SAXS traces of samples A-0 (= 300-5) and A-1 at α = 0 or 0.5. B = back, *i.e.* the data were recorded after a heating cycle. The black (or yellow) dotted lines are models fitting the data. B = back, *i.e.* the data were recorded at 25°C after heating to 80°C.

Table S8. Geometrical parameters of the PDMAc-*b*-P(MEA-*co*-AA) nano-objects obtained by PISA depending on α and the temperature by SAXS.

#	α	T (°C)	Morpho. SAXS[1]	D[2] (nm) (σ)	l or e (nm) (σ) [3]
300-5 (=A-0)	*0 (pristine)*	5	V	49 (1)	18 (0.10)
		25	V	70 (0.64)	24 (0.13)
		40	V	71 (0.69)	26 (0.10)
		80	V	130 (0.31)	48 (0.16)
	0.5	25	S	39 (0.09)	-
A-1	*1 (pristine)*	5	S	30 (0.10)	-
		25	S	37 (0.07)	-
		60	S	39 (0.11)	-
		80	S	46 (0.13)	-
		25 back	S	45 (0.14)	-
	0.5	25	S	51 (0.15)	-
		40	S	53 (0.12)	-
		60	V	80 (0.16)	24 (0.25)
	0	5	V	59 (0.32)	17 (0.07)
		25	V	61 (0.28)	21 (0.03)
		40	V	74 (0.30)	24 (0.06)
150-5	*0 (pristine)*	5	S	20 (0.08)	-
		25	S	27 (0.09)	-
		40	V	40 (0.41)	14 (0.09)
	0.5	25	S	21 (0.12)	-
150-30	*0 (pristine)*	5	S*	20 (0.15)	-
		25	F	18 (0.23)	> 100
		40	V	48 (1)	13 (0.16)
		80	L	-	80 (0.78)
		25 back	F	15 (0.41)	> 100

[1] Model used on SaSview to fit the SAXS experimental data. S = spheres, F = fibers, V = vesicles and L = lamellae. [2] Diameter D and its 'lognormal polydispersity' σ of either spheres, fibers or vesicles determined by fitting. [3] Length l (for cylinders), membrane thickness e (for vesicles or lamellae) and their 'lognormal polydispersity' σ determined by fitting. m = monodisperse.

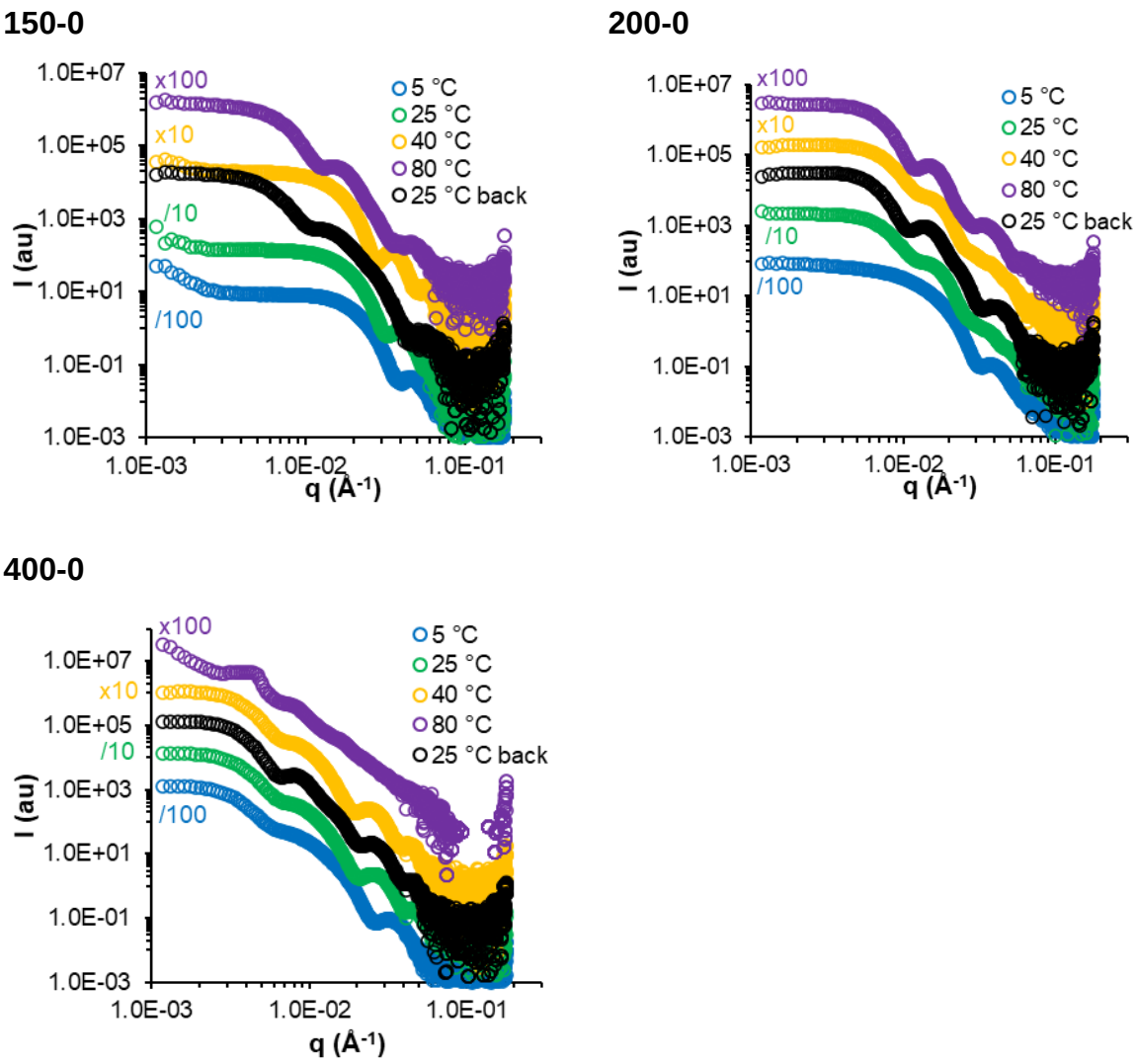

Figure S17. Temperature-controlled SAXS traces of samples 150-0, 200-0, 400-0. “back”: the data were recorded after one heating cycle and return to 25°C.

REFERENCES

[1] N. Audureau, C. Veith, F. Coumes, T. P. T. Nguyen, J. Rieger, F. Stoffelbach, *Macromol. Rapid Commun.* **2021**, *42*, 2100556.

[2] L. Couvreur, C. Lefay, J. Belleney, B. Charleux, O. Guerret, S. Magnet, *Macromolecules* **2003**, *36*, 8260–8267.

[3] D. F., Mexico, A. Rojas-Hernández, E. L. Ibarra-Montaño, N. Rodríguez-Laguna, A. Aníbal Sánchez-Hernández, *J. Appl. Sol. Chem. Model.* **2015**, *4*, 7–18.

[4] S. Recknagel, M. Breitenbach, J. Pautz, D. Lück, *Analytica Chimica Acta* **2007**, *599*, 256–263.

[5] M. Sedlák, Č. Koňák, P. Štěpánek, J. Jakeš, *Polymer* **1987**, *28*, 873–880.

[6] A. Guinier, G. Fournet, K. L. Yudowitch, *Small-Angle Scattering of X-Rays*, Wiley, **1955**.

[7] J. S. Pedersen, *J. Appl. Crystal.* **2000**, *33*, 637–640.

[8] C. Debrie, N. Coudert, J.-M. Guigner, T. Nicolai, F. Stoffelbach, O. Colombani, J. Rieger, *Angew. Chem. Internat. Ed.* **2023**, *62*, e202215134.

[9] S. Harrisson, F. Ercole, B. W. Muir, *Polym. Chem.* **2010**, *1*, 326–332.

[10] N. Audureau, F. Coumes, J.-M. Guigner, C. Guibert, F. Stoffelbach, J. Rieger, *Macromolecules* **2022**, *55*, 10993–11005.

[11] C. Debrie, N. Coudert, J. Abdul, S. Harrisson, O. Colombani, J. Rieger, *Macromolecules* **2023**, *56*, 8497–8506.

[12] J. Zhang, B. Farias-Mancilla, I. Kulai, S. Hoeppener, B. Lonetti, S. Prévost, J. Ulbrich, M. Destarac, O. Colombani, U. S. Schubert, C. Guerrero-Sanchez, S. Harrisson, *Angew. Chem. Int. Ed.* **2021**, *60*, 4925–4930.

[13] N. Coudert, C. Debrie, J. Rieger, T. Nicolai, O. Colombani, *Macromolecules* **2022**, *55*, 10502–10512.

[14] J. C. Foster, S. Varlas, B. Couturaud, J. R. Jones, R. Keogh, R. T. Mathers, R. K. O'Reilly, *Angew. Chem. Internat. Ed.* **2018**, *57*, 15733–15737.

[15] R. Hoogenboom, A.-M. Zorn, H. Keul, C. Barner-Kowollik, M. Moeller, *Polym. Chem.* **2012**, *3*, 335–342.

[16] L. Hou, K. Ma, Z. An, P. Wu, *Macromolecules* **2014**, *47*, 1144–1154.